Original Article

Adenovirus-mediated delivery of p27^{KIP1} to prevent wound healing after experimental glaucoma filtration surgery

Jian-gang YANG[1,*], Nai-xue SUN[1], Li-jun CUI[2], Xiao-hua WANG[1], Zhao-hui FENG[1]

[1]*Department of Ophthalmology, Second Affiliated Hospital of Medical School, Xi-an Jiaotong University;* [2]*Department of Ophthalmology, First Affiliated Hospital of Medical School, Xi-an Jiaotong University, Xi-an 710004, China*

Aim: The aim of the study was to evaluate the outcome of adenovirus-mediated p27^{KIP1} (Ad-p27) expression on wound healing after filtration surgery and to investigate the inhibition of cell proliferation induced by Ad-p27.
Methods: We constructed the adenovirus recombinant vector Ad-p27 and administered it to a rabbit model of glaucoma filtration surgery by subconjunctival injection; phosphate-buffered saline (PBS) and mitomycin C (MMC) were used as controls. Intraocular pressure (IOP), bleb scores, and anterior chamber depths were observed during a 28-d period. Histological examinations, fluorescence observations and Western blot analyses were evaluated.
Results: Ad-p27 enhanced the surgical outcome and inhibited cell proliferation when compared with PBS. Bleb scores in the Ad-p27-treated eyes were higher than those in the PBS-treated eyes on d 7 (P<0.01), 14 (P<0.01) and 21 (P<0.05). On d 28, IOP remained significantly decreased in the Ad-p27 group compared with the PBS group (P<0.05). However, no differences in bleb scores or IOPs were observed between the Ad-p27 and MMC groups. Histological analysis showed that total cell numbers were markedly reduced, and less scar tissue was observed at the surgical site in eyes treated with Ad-p27. The number of fibroblasts was decreased in Tenon's capsule in Ad-p27-treated eyes; however, a marked and diffuse signal from the green fluorescent protein (GFP) was observed in fibroblasts. Western blot analysis revealed a high level of p27^{KIP1} expression in conjunctival epithelium (P<0.01), relatively high expression in superficial scleral stroma (P<0.01), and low expression in corneal epithelium in the Ad-p27 group.
Conclusions: Ad-p27 administration significantly improves the outcome of filtration surgery and inhibits postoperative proliferation in rabbit eyes. These findings suggest that p27^{KIP1} is a potential adjunctive agent for inhibition of wound healing after filtration surgery.

Keywords: adenovirus; p27^{KIP1}; proliferation; glaucoma; surgery
Acta Pharmacologica Sinica (2009) 30: 413–423; doi: 10.1038/aps.2009.23

Introduction

Glaucoma filtration surgery is the most frequently used procedure applied to decrease the intraocular pressure (IOP) in cases of severe glaucoma. The procedure was designed to open a new route for drainage of the aqueous humor from the anterior chamber to the subconjunctival space. However, the long-term success of this approach is often impaired by excessive postoperative scarring at the wound site. The local use of antiproliferative agents, such as mitomycin C (MMC) and 5-fluorouracil (5-FU), has improved the surgery outcome by preventing cell growth and scar formation. However, the administration of these drugs can result in a variety of toxicities, including wound leakage, corneal erosion and, rarely, necrosis of the corneal stroma and iris, chronic hypotony, corneal stromal neovascularization, and scleral ulceration[1–4].

Cell cycle progression is regulated by a combination of positive and negative regulators. It is activated by a family of cyclins and cyclin-dependent kinases (CDKs). On the other hand, the CDK inhibitors (CKIs) negatively regulate progression of the cell cycle by inhibiting the activity of cyclin-CDK complexes. p27^{KIP1}, a member of the CKI family, plays a pivotal role in the control of cell proliferation. It inhibits the activities of the complexes CDK4-cyclin D, CDK6-cyclin D and CDK2-cyclin E, through direct interaction in the G_1/S transition[5–8]. However, p27^{KIP1} also promotes

* Correspondence to Dr Jian-gang YANG.
E-mail jgyang.xjtu@gmail.com
Received 2008-11-30 Accepted 2009-02-19

the assembly of CDK4-cyclin D and CDK6-cyclin D[9]. The level of $p27^{KIP1}$ is high during G_0 phase but decreases rapidly on reentry of the cells into G_1 phase[10]. This rapid removal of $p27^{KIP1}$ at the G_0/G_1 transition is required for effective progression of the cell cycle to S phase. In the S and G_2 phases, degradation of $p27^{KIP1}$ is promoted by phosphorylation of Thr^{187}, regulated by the cyclin E-CDK2 complex, and this reaction is required for binding of $p27^{KIP1}$ to Skp2, a F-box protein that is responsible for $p27^{KIP1}$ recognition[11, 12].

Cellular proliferation is regulated primarily by regulation of the cell cycle. A low level of $p27^{KIP1}$ expression was correlated with high proliferative and migratory capacity, whereas nuclear accumulation of this CKI was associated with a quiescent and static phenotype[13, 14]. This dual inhibitory function of $p27^{KIP1}$ was essential for the observation of blockade of CDK activity[13].

Gene delivery to Tenon's capsule fibroblasts by viral vectors is effective in inhibiting cell proliferation in several models of filtration surgery[15, 16]. The hypothesis of our study was that a recombinant $p27^{KIP1}$ would prevent wound healing in experimental filtration surgery. We investigated the effect of adenovirus-mediated $p27^{KIP1}$ (Ad-p27) on inhibition of cell proliferation and scarring in rabbit eyes.

Materials and methods

Cell lines and animals The 293 cell line was kindly provided by Dr Zeng-hui TENG (Fourth Military Medical University, China). These cells were maintained in Dulbecco's modified Eagle's medium (DMEM) supplemented with 10% fetal bovine serum (FBS), 0.1 $U{\cdot}L^{-1}$ of penicillin, and 100 $g{\cdot}L^{-1}$ of streptomycin at 37 °C in 5% CO_2.

A total of 57 adult albino rabbits weighing between 2 and 3 kg were used for the experiments. All animal procedures were performed in accordance with the ARVO Statement for the Use of Animals in Ophthalmic and Vision Research. These animals were used to evaluate the effect of Ad-p27 in filtration surgery. All experimental analyses using rabbits were conducted in a masked fashion, including surgery and the determination of histological features and $p27^{KIP}$ expression.

Construction of recombinant adenoviruses The $p27^{KIP1}$-expressing adenovirus Ad-p27 was constructed and validated according to standard techniques as previously described[17]. In brief, primers were designed according to the full-length human $p27^{KIP1}$ cDNA sequence (Genbank Accession, NM 004064.2). The forward primer, 5′-CGCGTCGACATGTCAAACGTGCGAGTGTC-3′, which contains a *Sal* I restriction site, and the reverse primer, containing *Hind*III and Flag sites, 5′-CCAAGCTTATTTATCGTCATCGTCTTTGTAGTCGTTTGACGTCTTCTGAGGC-3′, were synthesized by Tarara Biotechnology Co LTD (Dalian, China). The restriction sites were used for subcloning into a shuttle plasmid, pShuttle-GFP-CMV (SinoGenoMax Co, Ltd, China).

PCR was performed in a 2×10^{-5} L reaction mixture containing 1×reaction buffer [25 mmol/L Tris-HCl (pH 8.0), 3 mmol/L $MgCl_2$, 0.5 $g{\cdot}L^{-1}$ phosphate buffered saline (BSA), 10 mmol/L each deoxyribonucleoside triphosphate], 0.01 mmol/L forward and reverse primers, 1 U of *Taq* DNA polymerase (Tarara Biotechnology, Dalian, China) and templates. The amplification was performed on a LightCycler (Roche Diagnostics, Mannheim, Germany) under the following thermal program: initial denaturation (94 °C, 1 min), 30 cycles of 94 °C (30 s), 56 °C (30 s) and 68 °C (1 min), and final extension (68 °C, 6 min). After verifying amplification by agarose gel electrophoresis, the PCR products were purified using a Plasmid DNA Extraction Kit (Qiagen Co, Germany). The purified products were subcloned into the shuttle plasmid, pShuttle-GFP-CMV, by double digestion with *Sal*I and *Hind* III (New England Biolabs Inc, USA). The clones that had inserts were further tested by digestion with *Sal*I and *Hind*III, and were subsequently sequenced. The resulting adenovirus shuttle plasmid was named pShuttle-CMV-p27 (Figure 1A).

The pShuttle-CMV-p27 vector was electroporated into electrocompetent BJ5183 cells carrying the pAdEasy-1 vector and recombinants were isolated by antibiotics kanamycin. Once the desired constructs were confirmed by PCR analysis, plasmid DNA was electroporated into DH5A cells for large-scale amplification of the recombinant plasmid vector, pAd-p27 (Figure 1B).

Recombinant adenovirus supernate was cotransfected (calcium phosphate) with the plasmid pJM17 containing the adenoviral genome into 293 cells. Recombination of the expression cassettes from the shuttle plasmids into pJM17 yielded viral DNA of packageable-size that produced adenovirus capable of replicating in 293 cells. Transfected 293 cells were overlaid with agarose to permit isolation of individual virus plaques for 96 h. The expression of GFP was determined *in vitro* by observing green fluorescence in infected cells using a fluorescent microscope (Leica DM IRB, Leica Microsystems, Germany). After three freeze-thaw cycles, virus was purified from the cell lysates by ultracentrifugation in CsCl gradients and purification by Graham's method[18]. The light absorption of the purified virus at 260 nm was used to calculate the granule quantity and purity of the virus, using the expression virus titer $pfu{\cdot}L^{-1}=A_{260}\times dilution\times10^{15}$. The viral titer of Ad-p27 was 2.1×10^{15} $pfu{\cdot}L^{-1}$.

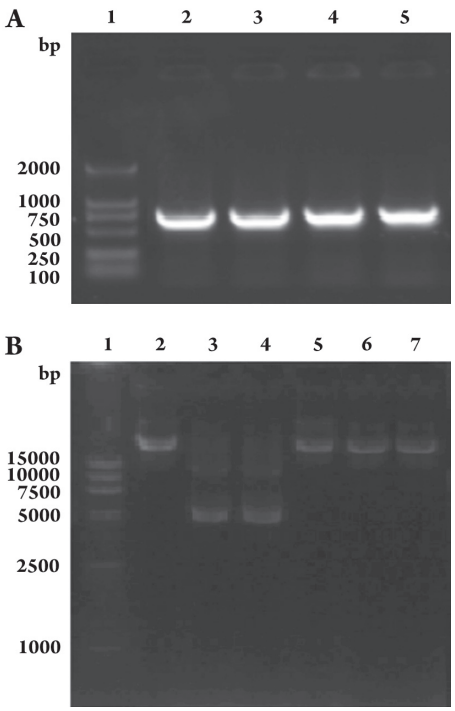

Figure 1. (A) PCR analysis of pShuttle-CMV-p27. 1: DNA marker; 2–5: pShuttle-CMV-p27. (B) Analysis of agarose gel electrophoresis for plasmid pAd-p27. 1: DNA marker, 2–7: electrophoresis photographs of pAd-p27. The positive clones include 2, 5, 6, and 7.

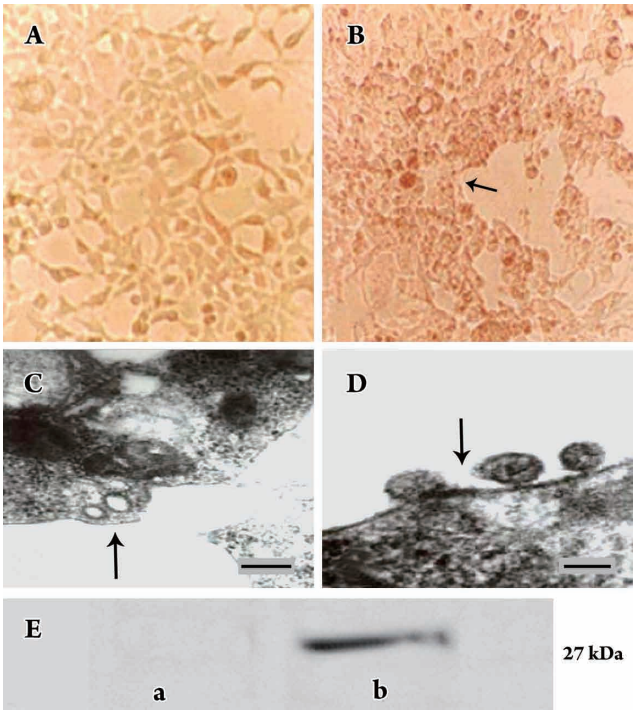

Figure 2. Recombination adenovirus assays in 293 cells. (A) Micrograph of normal 293 cells; (B) The formation of plaque (arrow). (C) The virus-like particles in 293 cells observed with TEM (arrow). (D) The pullulation of virus-like particles (arrow). Scale bar, (C) 0.2 μm; (D) 0.1 μm. (E) pAd-p27 transfection (b) and non-infection in adenovirus vector (a) by Western blots.

Recombination adenovirus assays The virus plaques were observed with a light microscope (Figure 2A, 2B). 293 cells infected with recombinant Ad-p27 (10^{10} particles) were cultured in 30-mm wells. Cells were then washed with PBS and incubated at 37 °C. When infected 293 cells showed evidence of cytopathic effects (CPE), the cells were harvested and observed with a transmission electron microscope (TEM; Philips EM 420, Netherland)(Figure 2C, 2D). Furthermore, we assayed Ad-p27 by Western blots (Figure 2E).

Construction of animal models and Ad-p27 delivery The surgical procedure was performed as previously described[19]. In brief, animals were anesthetized with an intramuscular injection of ketamine (7.5×10^{-3}–1.2×10^{-2} kg) and xylazine (1.2×10^{-2}–2.5×10^{-2} kg). Exposure of the eyeball was achieved with a wire lid speculum. A fornix-based flap of the conjunctiva and Tenon's capsule were raised in the superior nasal quadrant of either the left or the right eye, selected randomly. A limbus-based triangle scleral flap was outlined with a steel blade and carefully dissected. A stab knife (diameter, 1.5 mm) was then used to create the entry into the anterior chamber at the surgical limbus. Consequently, the tissue blocking the entrance was excised and a peripheral iridectomy was performed through the fistula. The flaps of sclera and conjunctiva were closed with an 8–0 nylon suture.

Ad-p27 of 8.0×10^{14} pfu·L^{-1} (1.0×10^{-4} L) was delivered to the conjunctiva by subconjunctival injection at the superonasal quadrant during surgery. Controls included animals dosed with PBS (negative control) and 0.02% MMC (Zhejiang Hisun Pharmaceutical Co, Ltd, China; positive control). After surgery, 1% atropine sulfate ophthalmic ointment, neomycin sulfate and dexamethasone were applied to the eye.

Clinical evaluation We performed clinical assessments within 28 d after surgery. The intraocular pressure (IOP) was measured with a Perkins handheld applanation tonometer (HL-2, Kowa, Nagoya, Japan). A slit lamp microscope was used for observations of filtration blebs and depth of the anterior chamber, and complications were recorded. Blebs were evaluated on a qualitative scale of 1+ to 4+, based on the bleb's appearance, size, and vascularity, and documented as described[20, 21]. The scores reflecting increasing bleb height and size were as follows: 1+, minimal height, conjunctiva thickening, and no microcysts; 2+, microcysts are present; 3+, elevated bleb covering 3 to 4 clock hours of the eye; and 4+, greatly elevated bleb covering more than 5 clock hours of

the eye. A score of 0 indicated no observable bleb.

Histological evaluation For light microscope analysis, animals were sacrificed on d 7, 14, 21, and 28 after filtration surgery. Eyes were enucleated, rinsed in PBS, and fixed in 4% paraformaldehyde. The tissue was embedded in mounting medium, and 5-μm thickness slices were mounted on slides and stained with hematoxylin and eosin.

For electron microscope, animals were sacrificed 28 d after surgery. Eyes were fixed with 0.5 L of a mixture containing 4% paraformaldehyde and 0.1% glutaraldehyde in 0.1 mol/L phosphate buffer for 30 min after enucleation. With the conjunctiva and Tenon's capsular thoroughly fixed, small pieces (1×1 mm) were cut from the central region of the surgical sites and rinsed in 2% glutaraldehyde in 0.1 mol/L cacodylate buffer (pH 7.4) at room temperature. The tissue was postfixed in 2% OsO_4, dehydrated, and embedded in epoxy resin. Ultrathin sections were stained with uranyl acetate and lead citrate and inspected with a transmission electron microscope.

Fluorescence microscopy Fluorescence was observed using a fluorescence microscope on d 28 after surgery. Glass slides and coverslips were used to mount the samples. An image of a single fluorescent virus particle was estimated; the particle was localized between the Ad-p27 group and the PBS group.

Western blot analysis Eyes treated with Ad-p27 or PBS were enucleated on d 28 after filtration surgery. Conjunctiva, sclera and corneas from the surgical site were excised. Conjunctival epithelial cells, corneal epithelial cells and scleral flaps were then peeled carefully, rinsed with 10 mL PBS, and collected by scraping with a spatula in 10^{-2} L of a cold medium containing 50 mmol/L 3-(N-morpholino)propanesulfonic acid (pH 7.0), 10 mmol/L NaF, 1 mmol/L EDTA, 0.3 mol/L sucrose, 0.4 mmol/L Pefabloc, 10^{-2} g·L^{-1} aprotinin, 2×10^{-3} g·L^{-1} leupeptin, and 10^{-3} g·L^{-1} pepstatin A. The cells were then sedimented by centrifugation at 2500×*g* for 2 min and stored at -70 °C. Within 14 d of storage, the frozen cells were thawed and homogenized in an ice-cold lysis buffer [10 mmol/L Tris-Cl, 1% sodium dodecyl sulfate (SDS) and 1 mmol/L Na_2VO_4, pH 7.4]. The homogenate was centrifuged at 8000×g for 30 min at 4 °C. The total protein concentration was determined by the bicinchoninic acid assay method (Pierce). The cell lysate was subjected to SDS-PAGE. The electrophoresed proteins were subsequently transferred to a polyvinylidene difluoride membrane. The primary antibodies used were rabbit monoclonal antibodies to $p27^{KIP1}$ (Santa Cruz Biotechnology Inc, Santa Cruz, USA). Reactions were visualized with a suitable secondary antibody conjugated with horseradish peroxidase using enhanced chemiluminescence reagents. β-actin (Sigma, St Louis, USA) served as the internal positive control for the Western blots.

Statistical analysis The software program SPSS 12.0 was utilized in our experiments. We applied the independent sample *t* test to evaluate data from IOP and Western blotting and the independent samples nonparametric test to analyze bleb scores. $P<0.05$ indicates a statistically significant difference.

Results

Outcomes of clinical evaluation A comparison of IOP measurements between the Ad-p27 group and the control (PBS or MMC) groups is illustrated in Figure 3. The baseline IOP was 23.8 mmHg in Ad-p27-treated eyes. After surgery, a steep reduction in IOP was observed in all groups. However, IOP in the PBS-treated eyes recovered rapidly on d 14. The eyes treated with Ad-p27 showed maintenance of low IOP through d 28. Compared with PBS, the hypotensive response induced by Ad-p27 significantly decreased on d 7 ($P<0.05$), 14 ($P<0.01$), 21 ($P<0.01$) and 28 ($P<0.05$). In contrast, no significant difference was noted between the Ad-p27 and MMC groups.

Bleb survival was observed by slit lamp examination during a 28-d period after treatment with Ad-p27. A bleb was judged to have failed if a flat, vascularized, scarred bleb was associated with a deep anterior chamber. In Ad-p27-treated eyes, the suppression of scarring maintained a translucent conjunctiva. Blebs with relatively thin walls were observed to be diffusely elevated within 14 d after surgery (Figure 4A, 4D) and became less elevated at later times. A cystic bleb formation was observed on d 28 (Figure 4G). Clinical examination showed that treatment with MMC was associated with elevated, diffuse blebs rather than flat, scarred, vascularized blebs within 14 d (Figure 4B, 4E). Furthermore, blebs with thin walls remained diffused, yet less elevated, until d 28 (Figure 4H). In contrast, blebs were observed to be elevated within 3 d in the PBS group. Blebs were less elevated and more vascularized in appearance on d 7 and flat on d 14 (Figure 4C, 4F). Scarring of the conjunctiva was prominent. Subconjunctival fibrotic tissue covered and impaired the view of the scleral flap. No bleb formation was detectable at d 21 after surgery (Figure 4I).

Blebs in eyes treated with Ad-p27 were not significant different in comparison with the matched controls within 3 d. However, the bleb scores of eyes treated with Ad-p27 were higher than the scores of the PBS-treated eyes after 7 d (Figure 4J). Statistical evaluation of the data showed significantly larger blebs for Ad-p27-treated eyes relative to the

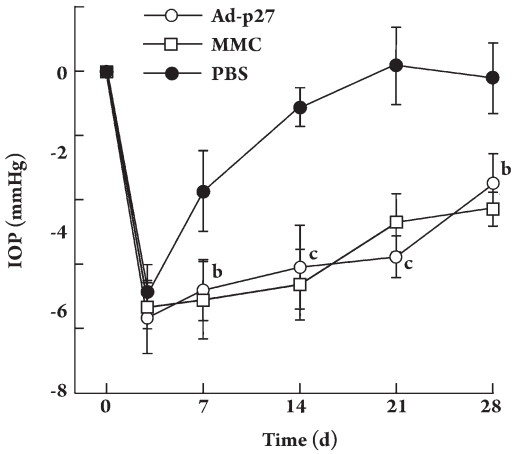

Figure 3. IOP of rabbits during a 28-d period treated with Ad-p27 *vs* controls (PBS or MMC) (n=6). Data are given as mean±SD. ^{b}P<0.05, ^{c}P<0.01 *vs* control.

eyes treated with PBS on d 7 (P<0.01), 14 (P<0.01), and 21 (P<0.05). On d 28, the bleb scores in Ad-p27-treated eyes were markedly decreased, and no difference was observed when comparing them with PBS-treated eyes. The analysis of bleb scores revealed no significant difference between the Ad-p27 and MMC groups during the 28-d period, although the scores in Ad-p27-treated eyes were slightly lower than those in MMC-treated eyes.

The depth of the anterior chamber was another indicator that indirectly implied aqueous humor outflow in the experiments. The anterior chambers were shallow within 3 d post-surgery and increasingly deepened among the experimental group and the two control groups. However, the anterior chambers were slightly shallower in Ad-p27-treated and MMC-treated eyes than those in PBS-treated eyes by d 7.

No obvious complications were observed in the Ad-p27-treated eyes within the 28 d period, such as bleb leaks, corneal epithelial defects, and hypotony, as assessed with a slit lamp microscope. However, hyphema occurred within 7 d in MMC-treated eyes.

Histological observation for inhibition of cell proliferation Histological analysis of the specimens was performed in samples collected from the center of the sclerectomy site. In the Ad-p27-treated eyes, a marked reduction was noted in subconjunctival scar tissue, and the total cellularity had decreased compared with that in the PBS-treated eyes.

Histological profiles revealed massive subconjunctival scarring in the PBS group. In the first 7 d, a cavity with thick walls was noted at the surgical site. The conjunctiva consisted of a goblet-cell-containing epithelium with an intact

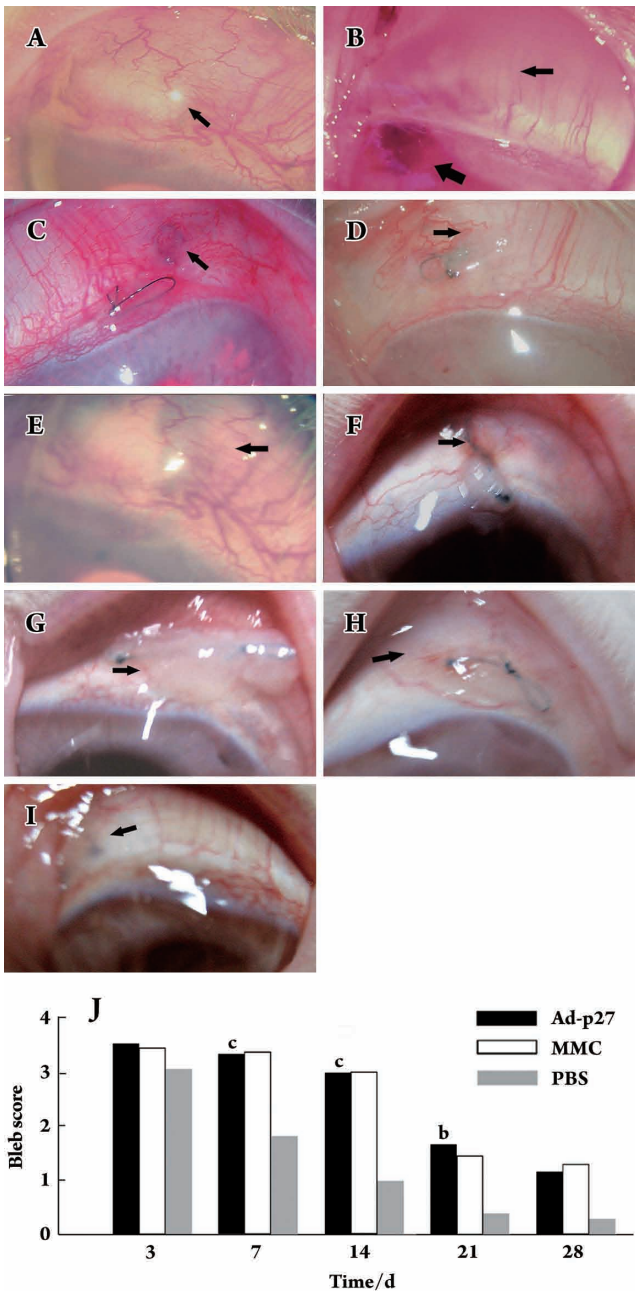

Figure 4. Bleb scores and morphology in rabbit eyes treated with Ad-p27 or controls within 28 d after surgery (n=6). The blebs (thin arrows) are observed among Ad-p27-treated, MMC-treated or PBS-treated group on d 7 (A, B, C), d 14 (D, E, F) and d 28 (G, H, I), respectively. The cystic bleb survived in the Ad-p27-treated group remains elevated on d 28 (E). The bleb with MMC treatment is diffusely elevated, yet hyphema occurs (thick arrow) within 7 d (B). On d 28, the bleb remains diffused, but is less elevated (H). The bleb, formed with PBS treatment, is less elevated and more vascularized in appearance on d 7 (C). A flat bleb is an example of the bleb that does not survive (F). The statistical difference is evaluated between Ad-p27 group and PBS group on d 7 (P=0.002), d 14 (P=0.000) and d 21 (P=0.028) after surgery. However, no significant difference of bleb scores is observed between Ad-p27 group and MMC group (J).

epithelial basement membrane. The sclerotomy site was infiltrated by hypercellular fibrotic tissue. On d 14, the cellularity remained increased at the surgical sites (Figure 5C). The numbers of goblet cells and epithelial cells were maintained at a high level. However, the size of the subconjunctival cavity decreased markedly. On d 21 and 28, the wounds still exhibited a hypocellular appearance. The subepithelial connective tissue consisted of a dense collagenous connective tissue. Tenon's capsular mainly consisted of dense fibrotic connective tissue. However, the number of epithelial cells and goblet cells decreased, compared with their numbers on d 14. The subconjunctival cavity had disappeared. Eyes treated with PBS exhibited nearly complete scarring over the sclerectomy site, including evidence of new collagen deposition in the scleral flap created by surgery(Figure 6C).

A hypercellular condition was noted in Ad-p27-treated eyes on d 7, consisting predominantly of epithelial cells, goblet cells and collagenous connective tissue. However, the proliferation was slightly weaker than that observed in eyes treated with PBS. The subconjunctival cavity was markedly, diffusely elevated. On d 14, scarring was notably inhibited by treatment with Ad-p27. A relatively thin epithelial layer had completely covered Tenon's capsule, in which the number of goblet cells had evidently decreased. Although the collagenous connective tissue was still relatively dense, the cavity was highly elevated (Figure 5A). The subconjunctival fibrotic tissue was lost on d 21. Eyes treated with Ad-p27 had minimal evidence of new collagen deposition in the sclera. Finally, surgical sites exhibited a hypocellular appearance on d 28. The subepithelial connective tissue was loosely arranged and contained histologically clear spaces. Furthermore, the eyes did not reveal intra- or extraocular inflammatory reactions (Figure 6A).

As expected, there was also a marked reduction in total cellularity associated with MMC treatment. Histological sections from the surgical site at d 14 showed a looser architecture with a visible conjunctiva and bleb formation with fewer collagen deposits than seen with Ad-p27 treatment (Figure 5B). Mild epithelial defects developed in a thin epithelial layer, in which the number of goblet cells had evidently decreased. On d 21 and 28, the surviving MMC-induced blebs remained as loose cell infiltrations without notable collagen deposition. However, the epithelial defects were further aggravated (Figure 6B), suggesting that MMC is associated with potential complications such as thin walls that are at risk of wound leakage and infection.

Outcomes of ultrastructure evaluation We used TEM to compare the characteristics of eyes treated with Ad-p27 and with controls. At the cellular level, TEM showed a cor-

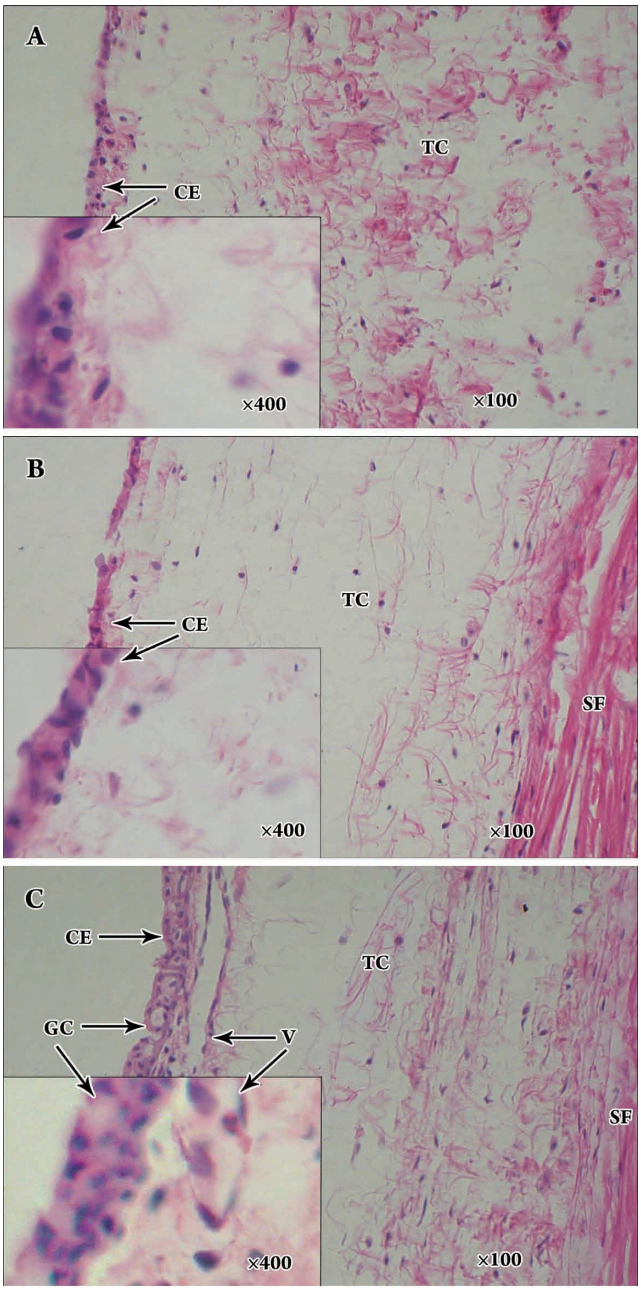

Figure 5. Histologic micrographs at surgical sites in rabbits between Ad-p27 group (A), MMC group (B) and PBS group (C) on day 14 after surgery (n=3). In Ad-p27 group, the conjunctival epithelium (CE) looks healthy, and consists of two or three layers of cells. The subepithelial connective tissues are relatively dense in Tenon's capsule (TC), and blood vessels (Vs) are plentiful. In MMC group, histological staining shows the hypocellular appearance of the subconjunctival bleb area. The mild defects are detected in the thin CE. In contrast, there is increased cellularity associated with PBS treatment. CE is thick between three and five cell layers in PBS group. There are plenty of subepithelial connective tissues and Vs in TC. The scleral flap (SF) attaches partially to the scleral (S) bed. There is a large quantity of goblet cells (GCs) in CE.

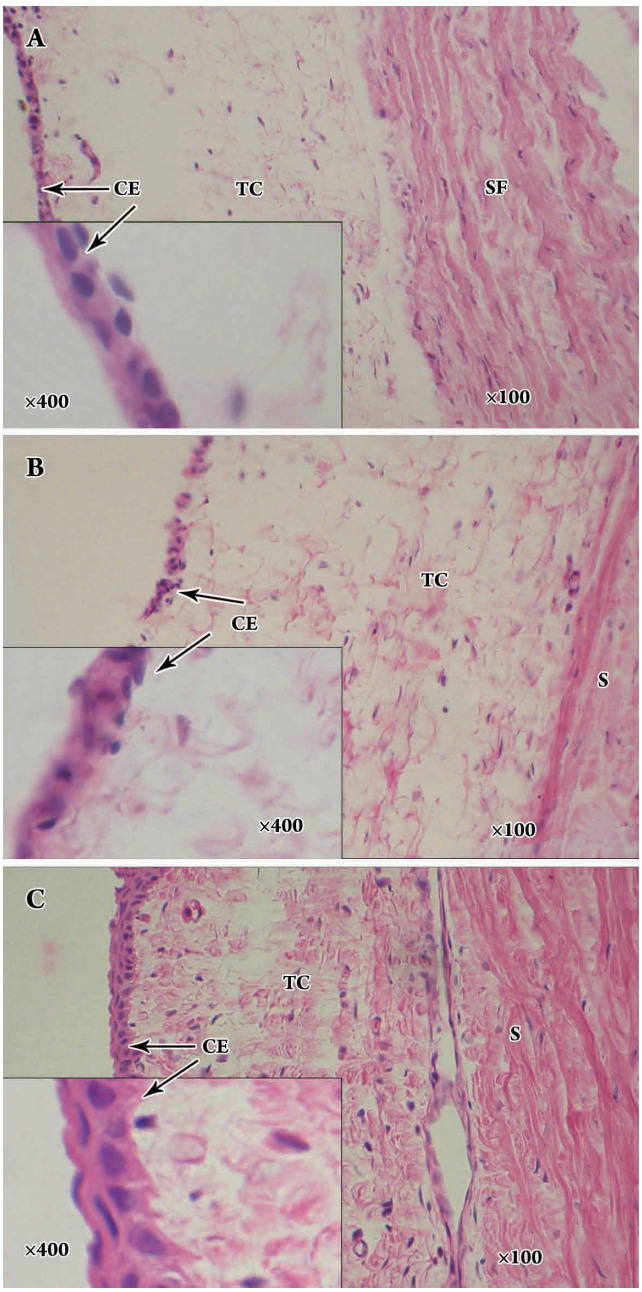

Figure 6. Histologic micrographs at surgical sites in rabbits between Ad-p27 group (A), MMC group (B) and PBS group (C) on d 28 (n=3). In Ad-p27 group, the conjunctival epithelium (CE) is thin only one or two layers of cells. The subepithelial connective tissues are loosed in Tenon's capsule (TC), with rare Vs. The space under scleral flap (SF) is clear, suggested that the filtering function via sclera is still maintained. In MMC group, the thin CE and loose subepithelial connective tissues are similar to those observed in Ad-p27 group. However, epithelial defects are aggravated. On the contrary, CE in bleb site is thick between two and four cell layers in PBS group. There are plenty of subepithelial connective tissues and Vs in TC. The SF has disappeared.

responding reduction in the number of conjunctival cells and formation of collagen fibrils in the Ad-p27-treated eyes.

In the eyes treated with Ad-p27, there was a substantial proportion of inactive conjunctival epithelial cells in which the cytoplasm was deeply stained. The active cells were mildly swollen, they contained enlarged mitochondria, and the intercellular space was widened (Figure 7A). The number of goblet cells was reduced. The cells contained vacuoles and enlarged mitochondria, some of which had degenerated (Figure 7B). This indicated that the secretion of mucin by the goblet cells was reduced, which rendered the ocular surface susceptible to environmental insults. There was a mild to moderate decrease of collagen density in the subepithelial area, intermixed with large amounts of an amorphous substance. Some fibroblasts were enlarged; they contained vacuoles in the cytoplasm and their mitochondria were swollen or dissolved (Figure 7C). Other fibroblasts displayed apoptotic features with cell shrinkage, deeply stained or dissolved cytoplasm, karyopyknosis and karyorrhexis, and unclear karyoplasm.

In eyes treated with MMC, TEM examination also revealed many inactive epithelial cells containing deeply stained cytoplasms and invaginated nuclei. The number of goblet cells was decreased. There was a reduction of collagen density in the subconjunctival sites. Fibroblasts progressed to widespread apoptotic cell death. The cells were shrunken, with dissolved cytoplasm, numerous karyopyknotic cells and occasional karyorrhexis.

In PBS-treated eyes, conjunctival epithelial cells were abundant with intact intercellular junctions, and the intercellular spaces were not enlarged. The cells contained normal amounts of rough endoplasmic reticulum and mitochondria in the cytoplasm and marked chromatospherites in the nuclei (Figure 7G). Subepithelial capillaries had multilaminar basement membranes. Goblet cells were tightly packed with mucus vacuoles. These cells also had well-developed, rough endoplasmic reticulum and Golgi, which contained a large number of secretory granules (Figure 7H). The fibroblasts were also plentiful, with functional organelles (Figure 7I).

GFP fluorescence analysis In order to identify Ad-p27-induced inhibition of postsurgical proliferation, we observed fibroblasts from surgical sites with a fluorescence microscope. On d 28 after surgery, the GFP-encoding $p27^{KIPI}$ fusion protein showed marked, diffused green fluorescence in fibroblasts from eyes treated with Ad-p27 (Figure 8A). There was no fluorescence in fibroblasts from eyes treated with PBS (Figure 8B).

Western blot assay for the $p27^{KIP1}$ protein Western blot analysis was performed to assess the expression of ade-

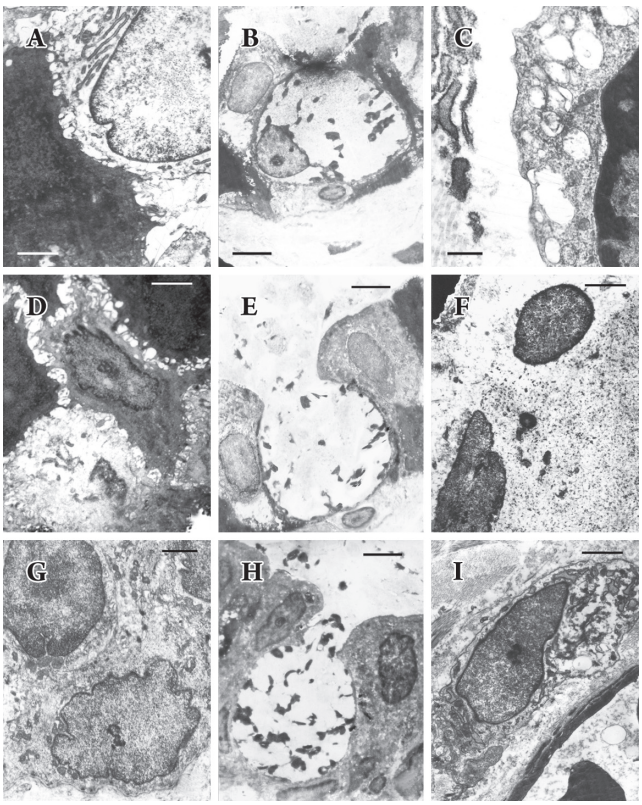

Figure 7. TEM photographs of conjunctiva treated with Ad-p27 (A, B, C), MMC (D, E, F) or PBS(G, H, I) (n=3). In Ad-p27-treated eyes, the inactive epithelial cell is enlarged (A). The fibroblastic cytoplasm is degenerated with swollen mitochondria and a plenty of vacuoles (C). The secretion of goblet cell decreased. The volume of neighboring epithelial cells is decreased, while the density is increased (B). In MMC group, the epithelial cells are inactive, and cytoplasm is deeply stained (D). The secretion of goblet cell decreases notably (E). The nuclei of fibroblast are round, and the cytoplasms are dissolved (F). In PBS-treated eyes, epithelial cells contain prominent, distended rough endoplasmic reticulums, and the intercellular junction is tight (G). The epithelial cells are arranged intactly with a relatively plenty of goblet cells which possessed secretion (H). Fibroblast is well-developed with clear euchromatin and chromatospherite. Collagen fiber bundles are arranged around fibroblast (I). Scale bar, (A, D, F, G, and I) 1 μm; (B, E, and H) 2 μm; (C) 0.5 μm.

novirus-encoded p27^{KIP1} in cell extracts prepared from conjunctival epithelium, corneal epithelium and stroma of scleral flaps on d 28 after surgery. Ad-p27 transfection induced high expression of p27^{KIP1} in conjunctival cells (P<0.01). In scleral cells of surgical sites, the expression of p27^{KIP1} in Ad-p27-treated eyes was also higher than that in PBS-treated eyes (P<0.01). However, the expression in the corneal cells was not significantly different (Figure 9).

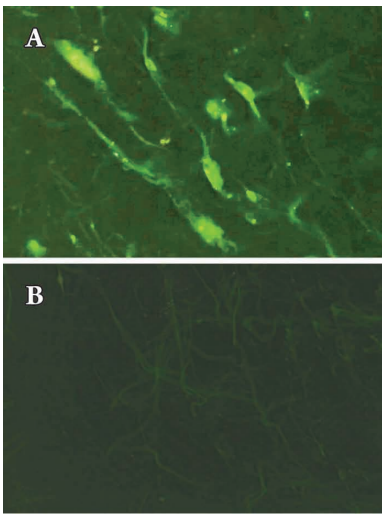

Figure 8. Fluorescence micrographs of GFP in fibroblasts stained in postsurgery (×400). Green fluorescence is markedly viewed in fibroblasts at surgical site treated with Ad-p27 (A), and no fluorescence is observed in eyes treated with PBS (B).

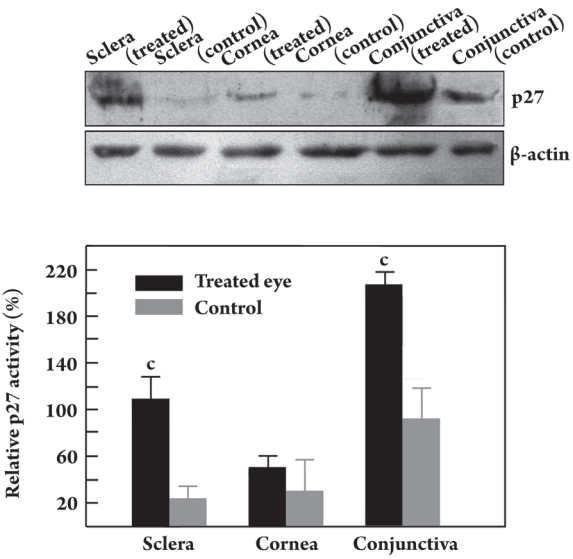

Figure 9. p27^{KIP1} differential expression in conjunctiva, cornea and superficial sclera at surgical sites treated with Ad-p27 compared with PBS (n=4). p27^{KIP1} protein levels are determined by Western blot and their densitometric values were normalized to β-actin. ^{c}P<0.01 *vs* control.

Discussion

Postoperative scarring is the main long-term problem in glaucoma filtration surgery. Surgical failure occurs because of scarring in the subconjunctival space by the ocular wound healing response. Modulation of the wound healing process to prevent excessive fibroblast proliferation and scar for-

mation can play a major role in improving the outcome of surgery. The process of wound healing consists of a complex cascade of interrelated events that include inflammation, extravasation of intravascular components, migration and proliferation of fibroblasts, extracellular matrix deposition, and scar formation[3, 19]. Antimetabolites that can inhibit DNA or RNA synthesis, cell division, protein synthesis, and fibroblast proliferation have been used as adjunctive therapy to prevent excessive scar formation in glaucoma surgery. The common clinical practice is to administer either 5-FU postoperatively by subconjunctival injection or MMC intraoperatively by local application. However, treatment with 5-FU and MMC is often associated with serious adverse effects, such as corneal epithelial defects, wound leaks, and hypotony with accompanying vision loss[1–4]. These problems have stimulated the search for alternative modes of drug delivery and new agents to minimize ocular complications.

CKIs block cell proliferation in wounded tissue by virtue of their ability to inhibit CDK-dependent phosphorylation of critical substrates in the G1 phase of the cell cycle. In previous studies, $p21^{CIP1}$ was utilized to prevent the failure of filtration surgery in rabbits. Both subconjunctival injection and topical treatment can deliver recombinant adenovirus containing the p21 gene (rAd-p21) to conjunctiva to prevent cell proliferation after glaucoma surgery[15, 22]. The vector rAd-p53 induced a marked overexpression of p53 in human Tenon's fibroblasts, leading to increased expression of $p21^{CIP1}$, which regulated wound healing following glaucoma surgery[16]. Other experiments have shown efficient expression of reporter genes (CAT and β-gal) in glaucoma surgery tissues (conjunctival fibroblasts) using plasmid or adenovirus constructs injected postoperatively into the filtering bleb[23].

Using Western blot experiments, we showed that the Ad-p27-induced inhibition of proliferation was associated with a significant up-regulation of $p27^{KIP1}$ expression in conjunctival epithelial cells from surgical sites. On the contrary, low expression of $p27^{KIP1}$ was related to significant proliferation in eyes treated with PBS[24]. In addition, $p27^{KIP1}$ expression in superficial scleral stroma of Ad-p27-treated eyes was higher than that of PBS-treated eyes, although the level decreased notably compared with that in conjunctival epithelial cells. These findings indicate that Ad-p27 was delivered to the subflap of the sclera, where it inhibited fibroblast proliferation and delayed wound healing. In previous studies, Yoshida *et al* suggested that the disappearance of $p27^{KIP1}$ was well-correlated with cell proliferation in the corneal epithelium after injury[25]. CDK4 and p27 regulate proliferation in corneal endothelial cells by regulating the cell cycle progression[26]. Our experiments showed that $p27^{KIP1}$ expression did not increase in the corneal epithelium of Ad-p27-treated eyes, which suggested that the mode of Ad-p27 delivery was localized at the surgical sites of glaucoma filtration.

Rabbit models of filtration surgery, although commonly used experimentally, present a very aggressive scarring response compared with that in humans. Therefore, most agents shown to reduce scar formation in the rabbit are effective in humans[27]. The present study demonstrated the efficacy of Ad-p27 as an adjunct in promoting the success of filtration surgery in rabbit eyes. IOP was used as a critical indicator for antiproliferative treatments. Eyes that received Ad-p27 after surgery had lowered IOP for at least 28 d. The histological findings of blebs and anterior chamber depth supported this outcome of hypotensive response in the experimental eyes.

In this study, Ad-p27 was effective in improving bleb survival and surgical outcome. Bleb formation and anterior chamber depth were chosen as indirect indicators of the drainage of fluid through the tube into the subconjunctival space. In most animals, the anterior chamber was flat on d 3 and gradually deepened in the following days. The anterior chambers were slightly flatter in Ad-p27-treated eyes than those in PBS-treated eyes. Ad-p27 treatment resulted in well-formed bleb cavities. Whereas the PBS-induced blebs typically failed, no change in outflow facility was noted for eyes treated with Ad-p27. However, differences were not observed between the Ad-p27 and MMC groups during the 28-d period. The alteration of blebs and anterior chambers was consistent with the outcomes of IOP. According to the results of this study, Ad-p27 can be considered as a potentially optimized anti-scarring agent in filtration surgery without any obvious complications. In contrast, the epithelial defects on the MMC-induced blebs probably caused severe complications such as wound leakage, although the blebs remained significantly thin and diffuse.

Histologically, the blebs from Ad-p27-treated eyes were prone to having relatively thin and cystic walls. In contrast, PBS-treated blebs appeared significantly thick walled, much more cystic, and more vascular. The conjunctival changes were examined by both light microscopy and electron microscopy. The blebs displayed a cell decrease in the subconjunctival and conjunctival layers at the site of sclerectomy. In a previous study, proliferation and activation of conjunctival fibroblasts play important roles in scarring after filtration surgery[28]. Our data show that Ad-p27 reduces activation of fibroblasts and increases apoptosis. Controlling fibroblast proliferation by delivery of Ad-p27 to conjunctival fibroblasts would therefore target the proliferative component of the wound healing response. Histological observations indi-

cate that Ad-p27 attenuates fibroproliferation and scarring in the rabbit model at a level comparable to that in PBS-treated eyes.

This demonstration of the use of $p27^{KIP1}$ in rabbit models of glaucoma filtration surgery represents an exciting new field for the development of agents for the inhibition of postsurgical scarring in the eye, without the severe side effects associated with existing modulating agents.

Acknowledgements

The authors thank Dr Yu-mei TIAN (Research Center for Neuroscience, Xi-an Jiaotong University) for technical support in this study.

Author contribution

Jian-gang Yang, Nai-xue SUN designed research; Li-jun CUI performed research; Xiao-hua WANG contributed new reagents or analytic tools; Zhao-hui FENG analyzed data; Jian-gang YANG wrote the paper.

References

1 Morris DA, Peracha MO, Shin DH, Kim C, Cha SC, Kim YY. Risk factors for early filtration failure requiring suture release after primary glaucoma triple procedure with adjunctive mitomycin. Arch Ophthalmol 1999; 117: 1149–54.
2 Esson DW, Neelakantan A, Iyer SA, Blalock TD, Balasubramanian L, Grotendorst GR, *et al*. Expression of connective tissue growth factor after glaucoma filtration surgery in a rabbit model. Invest Ophthalmol Vis Sci 2004; 45: 485–91.
3 Cordeiro MF, Gay JA, Khaw PT. Human anti-transforming growth factor-beta2 antibody: a new glaucoma anti-scarring agent. Invest Ophthalmol Vis Sci 1999; 40: 2225–34.
4 DeBry PW, Perkins TW, Heatley G, Kaufman P, Brumback LC. Incidence of late-onset bleb-related complications following trabeculectomy with mitomycin. Arch Ophthalmol 2002; 120: 297–300.
5 Sheaff RJ, Groudine M, Gordon M, Roberts JM, Clurman BE. Cyclin E-CDK2 is a regulator of $p27^{Kip1}$. Genes Dev 1997; 11: 1464–78.
6 Obaya AJ, Kotenko I, Cole MD, Sedivy JM. The proto-oncogene c-myc acts through the cyclin-dependent kinase (Cdk) inhibitor $p27^{Kip1}$ to facilitate the activation of Cdk4/6 and early G(1) phase progression. J Biol Chem 2002; 277: 31263–9.
7 Zhang W, Bergamaschi D, Jin B, Lu X. Posttranslational modifications of $p27^{kip1}$ determine its binding specificity to different cyclins and cyclin-dependent kinases *in vivo*. Blood 2005; 105: 3691–8.
8 Baldassarre G, Boccia A, Bruni P, Sandomenico C, Barone MV, Pepe S, *et al*. Retinoic acid induces neuronal differentiation of embryonal carcinoma cells by reducing proteasome-dependent proteolysis of the cyclin-dependent inhibitor p27. Cell Growth Differ 2000; 11: 517.
9 Lane HA, Beuvink I, Motoyama AB, Daly JM, Neve RM, Hynes NE. ErbB2 potentiates breast tumor proliferation through modulation of $p27^{Kip1}$-Cdk2 complex formation: receptor overexpression does not determine growth dependency. Mol Cell Biol 2000; 20: 3210–23.
10 Hara T, Kamura T, Kotoshiba S, Takahashi H, Fujiwara K, Onoyama I, *et al*. Role of the UBL-UBA protein KPC2 in degradation of p27 at G1 phase of the cell cycle. Mol Cell Biol 2005; 25: 9292–303.
11 Sabile A, Meyer AM, Wirbelauer C, Hess D, Kogel U, Scheffner M, *et al*. Regulation of p27 degradation and S-phase progression by Ro52 RING finger protein. Mol Cell Biol 2006; 26: 5994–6004.
12 St Croix B, Sheehan C, Rak JW, Flørenes VA, Slingerland JM, Kerbel RS. E-Cadherin-dependent growth suppression is mediated by the cyclin-dependent kinase inhibitor p27(KIP1). J Cell Biol 1998; 142: 557–71.
13 Fredersdorf S, Burns J, Milne AM, Packham G, Fallis L, Gillett CE, *et al*. High level expression of $p27^{kip1}$ and cyclin D1 in some human breast cancer cells: Inverse correlation between the expression of $p27^{kip1}$ and degree of malignancy in human breast and colorectal cancers. Proc Natl Acad Sci USA 1997; 94: 6380–5.
14 Masuda TA, Inoue H, Sonoda H, Mine S, Yoshikawa Y, Nakayama K, *et al*. Clinical and biological significance of S-phase kinase-associated protein 2 (Skp2) gene expression in gastric carcinoma: modulation of malignant phenotype by Skp2 overexpression, possibly via p27 proteolysis. Cancer Res 2002; 62: 3819–25.
15 Perkins TW, Faha B, Ni M, Kiland JA, Poulsen GL, Antelman D, *et al*. Adenovirus-mediated gene therapy using human p21WAF-1/Cip-1 to prevent wound healing in a rabbit model of glaucoma filtration surgery. Arch Ophthalmol 2002; 120: 941–9.
16 Johnson KT, Rödicker F, Heise K, Heinz C, Steuhl KP, Pützer BM, *et al*. Adenoviral p53 gene transfer inhibits human Tenon's capsule fibroblast proliferation. Br J Ophthalmol 2005; 89: 508–12.
17 Bryant P, Zheng Q, Pumiglia K. Focal adhesion kinase controls cellular levels of p27/Kip1 and p21/Cip1 through Skp2-dependent and -independent mechanisms. Mol Cell Biol 2006; 26: 4201–13.
18 Zhang X, Liu S, Liang C, Yang H. Adenovirus-mediated Rb gene transfect for head and neck cancer. Huaxi Yike Daxue Xuebao 2001; 32: 194–5. Chinese.
19 Grisanti S, Szurman P, Warga M, Kaczmarek R, Ziemssen F, Tatar O, *et al*. Decorin modulates wound healing in experimental glaucoma filtration surgery: a pilot study. Invest Ophthalmol Vis Sci 2005; 46: 191–6.
20 Perkins TW, Faha B, Ni M, Kiland JA, Poulsen GL, Antelman D, *et al*. Adenovirus-mediated gene therapy using human $p21^{WAF-1}$/Cip-1 to prevent wound healing in a rabbit model of glaucoma filtration surgery. Arch Ophthalmol. 2002; 120: 941–9.
21 Wong TT, Mead AL, Khaw PT. Matrix metalloproteinase inhibition modulates postoperative scarring after experimental glaucoma filtration surgery. Invest Ophthalmol Vis Sci 2003; 44: 1097–103.
22 Wen SF, Chen Z, Nery J, Faha B. Characterization of adenovirus p21 gene transfer, biodistribution, and immune response after local ocular delivery in New Zealand white rabbits. Exp Eye Res 2003; 77: 355–65.
23 Angella GJ, Sherwood MB, Balasubramanian L, Doyle JW, Smith MF, van Setten G, *et al*. Enhanced short-term plasmid transfection of filtration surgery tissues. Invest Ophthalmol Vis Sci 2000; 41:

4158–62.
24 Meyers JR, Corwin JT. Shape change controls supporting cell proliferation in lesioned mammalian balance epithelium. J Neurosci 2007; 27: 4313–25.
25 Yoshida K, Nakayama K, Nagahama H, Harada T, Harada C, Imaki J, *et al*. Involvement of p27(KIP1) degradation by Skp2 in the regulation of proliferation in response to wounding of corneal epithelium. Invest Ophthalmol Vis Sci 2002; 43: 364–70.
26 Lee HT, Kay EP. Regulatory role of PI3-kinase on expression of Cdk4 and p27, nuclear localization of Cdk4, and phosphorylation of p27 in corneal endothelial cells. Invest Ophthalmol Vis Sci 2003; 44: 1521–8.
27 Khaw PT, Doyle JW, Sherwood MB, Smith MF, McGorray S. Effects of intraoperative 5-fluorouracil or mitomycin C on glaucoma filtration surgery in the rabbit. Ophthalmology 1993; 100: 367–72.
28 Skuta GL, Parrish RK 2nd. Wound healing in glaucoma filtering surgery. Surv Ophthalmol 1987; 32: 149–70.